

Accounts

Electrochemical Instability in Liquid–Liquid Two-Phase Systems

Yuki Kitazumi and Takashi Kakiuchi*

Department of Energy and Hydrocarbon Chemistry, Graduate School of Engineering, Kyoto University, Kyoto 615-8510

Received July 19, 2011; E-mail: kakiuchi@scl.kyoto-u.ac.jp

On the basis of the dependency of adsorption and partitioning of ionic surfactant on the phase-boundary potential ($\Delta_{\mathrm{O}}^{\mathrm{W}}\phi$), it is possible to understand in a unified manner various instability phenomena at the liquid|liquid interface in the presence of ionic surfactants, such as spontaneous emulsification, oscillation of $\Delta_{\mathrm{O}}^{\mathrm{W}}\phi$ and interfacial tension, and irregularly increased currents on voltammograms of the transfer of surface-active ions across the interface. These instabilities are associated with the electrochemical instability, which defines a thermodynamically unstable condition at the liquid|liquid interface in terms of $\Delta_{\mathrm{O}}^{\mathrm{W}}\phi$ and is a fundamental concept to understand the instabilities in the presence of ionic surfactants. The characteristic manifestations of the electrochemical instability, that is, the irregularly increased current on voltammograms in the transfer of surface-active ions, the spontaneous emulsification, and the spontaneous oscillation of $\Delta_{\mathrm{O}}^{\mathrm{W}}\phi$ can be designed based on the criterion of the electrochemical instability.

1. Introduction

The instability at the interface between two immiscible solutions, such as an oil (O)|water (W) interface, is important in a variety of chemical processes, for example, dispersion, extraction, mixing, and separation. Counterintuitive phenomena, such as spontaneous emulsification[1–25] and oscillations of the meniscus,[26–28] interfacial tension (γ),[26–32] and phase-boundary potential ($\Delta_{\mathrm{O}}^{\mathrm{W}}\phi$)[26,28,30,31,33–42] at the liquid|liquid interface, are frequently encountered in many branches of chemistry and chemical engineering. Aside from the curiosity, these instabilities are of practical importance in chemical industry. For example, the extraction efficiency markedly increases by the spontaneous agitation of the interface and adjacent two immiscible solutions,[43,44] or, conversely, the separation of the mixture into two phases becomes difficult because of the stability of formed emulsions.[4] The control of the instability is hence desirable and useful in many applications of the liquid–liquid two-phase systems. However, our understanding of such interfacial instability is still limited, as Nishimi and Miller put it in 2000 "the challenge is to understand the mechanism of spontaneous emulsification."[19]

The electrochemical instability,[45] the concept which relates the instability at the liquid|liquid interface to $\Delta_{\mathrm{O}}^{\mathrm{W}}\phi$ and potential-dependent adsorption and partition of ionic surfactant, is presumed to play a pivotal role to explain why, when, and how the instability commences and ceases. This account summarizes the salient features of the electrochemical instability and aims to give an overview of the recent developments in the study of the electrochemical instability at the liquid|liquid interface.

2. A Historical Perspective

Spontaneous emulsification is an intriguing subject known for a long time and was addressed by Gad in 1878 in view of scientific curiosity.[1] This phenomenon has been tackled by many researchers[1–25,46] from curiosity and its importance in surface chemistry and related applications, such as dispersion of chemicals in industrial and agricultural processes,[7,21,43,44] drug delivery systems,[9,14,21] and the digestion of food in our body.[5] The fact that many hypotheses have been proposed over one hundred years for the mechanism of spontaneous emulsification attests that the mechanism is not fully explained yet. The models so far proposed include interfacial turbulence,[2,12] ultralow γ,[46] diffusion and stranding,[3,7,17] and differences in osmotic pressure.[10]

The oscillation phenomena are well-known at the liquid|liquid interface. Early studies of the oscillation at the interface have been carried out at the mercury|solution interface since the 1850s.[47–49] For example, Lippmann's beating heart is a classical oscillation system at the interface between mercury and an aqueous chromic acid solution when an iron needle touched the mercury.[48] At the O|W interface, the oscillations of $\Delta_{\mathrm{O}}^{\mathrm{W}}\phi$ and γ were studied from the 1970s.[26–41] The spontaneous emulsification and the oscillation phenomena often accompany the movement of the interface due to the Marangoni effect.[2,6,12,16,19,21,26–32,41] The Marangoni instability in a liquid–liquid two-phase system due to the transfer of a solute was first analyzed by Sternling and Scriven.[50] They determined the condition for the onset of the instability when a small perturbation was introduced into the system by the linear stability analysis. The model has been refined by taking into

Published on the web November 29, 2011; doi:10.1246/bcsj.20110217

account the nonsteady diffusion,[51] the Gibbs adsorption layer,[52] the surface elasticity,[53] the interfacial reaction,[54] the finite width of the system,[55] and the dissolution of solvent.[56] The stability of the system was characterized by a dimensionless parameter, the Marangoni number, which expresses the relative importance of the surface tension forces and the viscous forces at the interface.[52,55–58] The Marangoni instability continues while the Marangoni number is greater than its critical value. However, the reason why the system falls into the unstable state and jumps out of it has remained unclear.

Electrochemical aspects are of decisive importance in understanding and controlling the interfacial instability, because any interface is always electrically charged unless it is fortuitously or intentionally set to zero[59,60] and the interactions between the ions or redox active species and the charged interface seem to play a crucial role in the interfacial instability.[26,28,30,31,33–42,48] Since the early time of electroanalytical chemistry, the regularly irregular augmentation of the currents on polarograms beyond the level of diffusion-limited current, called polarographic maxima, was investigated.[61–68] Shikata suggested that the origin of the polarographic maximum in the reduction of nitrobenzene was the adsorption and desorption of nitrobenzene depending on the applied potential.[61] A photographic technique elucidated in detail the movement of the solution around a dropping mercury electrode.[64] It was proposed that the movement was induced by the heterogeneity of the current density on the surface of a dropping mercury electrode.[65–68] However, even at a stationary mercury pool electrode,[69,70] the polarographic maxima appear. Moreover, this type of model based on the hydrodynamics cannot explain why the polarographic maximum appears in a certain potential region near the half-wave potential. Recently, the unstable phenomena at the mercury electrode have been revisited using hanging mercury drop electrodes in molecular solvents and ionic liquids,[71–74] but the origin of the instability has been left unexplained.

In electrochemistry at the O|W interface,[75–78] the observed oscillation of $\Delta_O^W\phi$[26,28,30,31,33–42] has been explained in terms of the formation and destruction of the surfactant layer at the interface[33,35,38] or the adsorption and desorption of the ion-pair at the interface.[34,37,40] These models address the behavior under the unstable condition, but are not concerned with the fact that the irregularly augmented current appears only in a certain potential region on voltammograms in the ion transfer across the interface.[34,37,40,79–88]

A model based on the kinetics of ion-transfer, adsorption, and desorption reactions at the interface was proposed to explain the irregular current in a certain potential region on ion-transfer voltammograms.[89] However, this model disagrees with the irregular current on the potential-step chronoamperogram for the transfer of surface-active ions,[82,83,86,88] since the model assumes the steady-state current when the potential is kept constant.

The electrochemical instability proposed in 2002[45] defines the thermodynamic criterion of the unstable condition at the electrified liquid|liquid interface and explains why the interface becomes unstable and the unstable phenomena at the liquid|liquid interface appear in a certain limited potential region.

3. Potential-Dependent Adsorption of Surface-Active Ions at the Liquid|Liquid Interface

Electrochemical instability[45] is caused by the interplay of the potential-dependent adsorption of surface-active ions at the liquid|liquid interface and its partition between the two phases. To introduce the concept of the electrochemical instability, the potential-dependent adsorption is briefly described.

For the adsorption of an ionic species, i, at the O|W interface, adsorption may take place from both sides of the interface. The simplest model[90] that describes the potential-dependence of the standard Gibbs energy for the adsorption of i from phase α (=O or W), $\Delta G^{\alpha,0}_{ads,i}$, is written as,

$$\Delta G^{O,0}_{ads,i} = \Delta G^{\ominus}_{ads,i} + z_i F\beta_i[\Delta_O^W\phi - \Delta_O^W\phi_i^{\ominus}] \quad (1)$$

and

$$\Delta G^{W,0}_{ads,i} = \Delta G^{\ominus}_{ads,i} - z_i F(1-\beta_i)[\Delta_O^W\phi - \Delta_O^W\phi_i^{\ominus}] \quad (2)$$

where $\Delta_O^W\phi_i^{\ominus}$, β_i, z_i, $\Delta G^{\ominus}_{ads,i}$, and F are the standard ion-transfer potential of i, the potential-independent parameter having a value in the range, $0 < \beta_i < 1$, the charge of i, the standard Gibbs energy for the adsorption at $\Delta_O^W\phi_i^{\ominus}$, and the Faraday constant, respectively. Here, $\Delta_O^W\phi$ is defined as the electrostatic potential of W with respect to that of O. This model well describes the experimentally determined adsorption Gibbs energies of cetyltrimethylammonium at the nitrobenzene|W interface when the ions are distributed into the nitrobenzene phase[91,92] and decylammonium and decyl sulfate at the 1,2-dichloroethane (DCE)|W interface when the ions are distributed into the W phase.[87] Equations 1 and 2 are similar to the model of ion adsorption on the mercury electrode, which linearly depends on the surface charge density,[93,94] to the liquid|liquid interface.

Figure 1 shows the potential dependence of the surface coverage of i, θ_i, assuming the Frumkin isotherm, $B_i^{\alpha}c_i^{\alpha} = \theta_i/(1-\theta_i)\exp(-2a\theta_i)$, where $B_i^{\alpha} = \exp[-\Delta G^{\alpha,0}_{ads,i}/(RT)]$ is the adsorption coefficient of i from phase α, c_i^{α} is the bulk

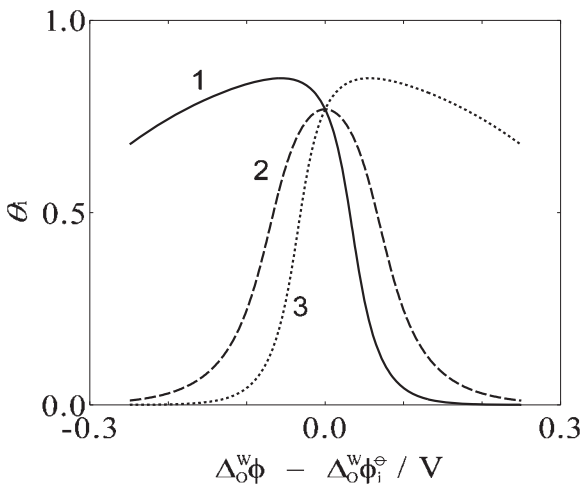

Figure 1. Potential dependencies of the surface coverage of surface-active ion having $\beta_i = 0.9$ (curve 1), 0.5 (curve 2), and 0.1 (curve 3) at the liquid|liquid interface assuming the Frumkin isotherm, when $\Delta G^{\ominus}_{ads,i} = -18\,\mathrm{kJ\,mol^{-1}}$, $z_i = 1$, $c_i^W + c_i^O = 1\,\mathrm{mmol\,dm^{-3}}$, and $a = 1$.

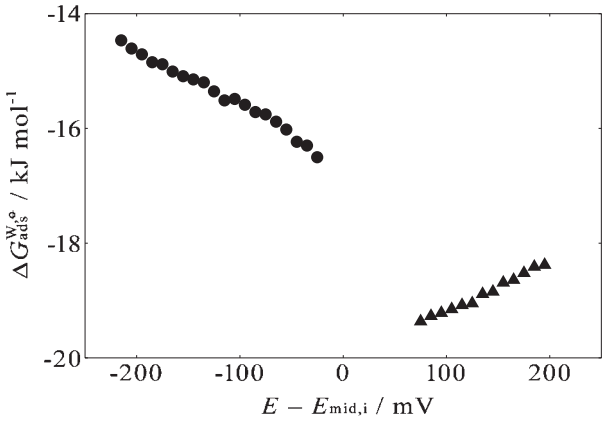

Figure 2. Potential dependences of the standard Gibbs energy for the adsorption of decylammonium (circles) and decyl sulfate (triangles) from W at the DCE|W interface. $E - E_{mid,i}$ indicates the potential with respect to the midpoint potential of the voltammogram for the transfer of each ion. Adapted from Ref. 87 with permission.

concentration of i in phase α, R is the gas constant, T is the temperature, and a is the interaction parameter. The curves in Figure 1 were calculated when $\Delta G^{\circ}_{ads,i} = -18\,\mathrm{kJ\,mol^{-1}}$, $a = 1$, $z_i = 1$ and $c_i^W + c_i^O = 1\,\mathrm{mmol\,dm^{-3}}$ at $\beta_i = 0.9$ (curve 1), 0.5 (curve 2), and 0.1 (curve 3). Curve 2 in Figure 1 has a maximum at $\Delta_O^W\phi_i^{\circ}$. The location of the maximum shifts to $\Delta_O^W\phi = \Delta_O^W\phi_i^{\circ} - 56\,\mathrm{mV}$ ($\Delta_O^W\phi = \Delta_O^W\phi_i^{\circ} + 56\,\mathrm{mV}$) in curve 1 (curve 3). A characteristic feature of the potential-dependent adsorption of surface-active ions is that the adsorbed amount of surface-active ions takes a maximum around $\Delta_O^W\phi_i^{\circ}$.[90]

A cation mainly distributes in the W phase when $\Delta_O^W\phi < \Delta_O^W\phi_i^{\circ}$. Figure 1 shows that an ionic surfactant having a high (low) β_i value ($0.5 \ll (\gg)\beta_i$) strongly (weakly) adsorbs at the interface from W in the potential where the ion is mainly distributed in W.

Figure 2 shows the experimentally determined $\Delta G^{W,0}_{ads,i}$ of decylammonium (circles) and decyl sulfate (triangles) at the DCE|W interface,[87] where $E_{mid,i}$ is the midpoint potential between the peaks in the forward and reverse scans of the transfer voltammogram for each ion. These values of $\Delta G^{W,0}_{ads,i}$ are linearly dependent on $\Delta_O^W\phi$. The slopes of the curves were -9.8 and $9.1\,\mathrm{kJ\,mol^{-1}\,V^{-1}}$ for decylammonium and decyl sulfate, respectively. The β_i values of decylammonium and decyl sulfate obtained from these plots are then 0.90 and 0.91, respectively.[87] Generally, surface-active ions having a charged hydrophilic moiety and an uncharged hydrophobic moiety, such as alkyl sulfates, alkylammoniums, alkanesulfonates, or carboxylates, have such a higher β value.[87]

4. The Concept of the Electrochemical Instability

Electrocapillary curves, that is, γ vs. $\Delta_O^W\phi$ curves, at the O|W interface are usually convex-upward parabolas.[91,92,95–99] In a polarized electrochemical liquid–liquid two-phase system, where $\Delta_O^W\phi$ is controlled externally, the cell is represented by:

$$\mathrm{RE1|O|W|RE2} \tag{3}$$

where RE1 and RE2 are the reference electrodes which are reversible to one of the ions in O and W, respectively. The potential of RE2 with respect to that of RE1 is denoted as E. E is equal to $\Delta_O^W\phi + E_{ref}$, where E_{ref} is the sum of the potentials of the reference electrodes.[100] According to the Lippmann equation,[101] the slope of the electrocapillary curve gives the excess surface charge density on the W side of the interface, q^W,

$$q^W = -\left(\frac{\partial\gamma}{\partial E}\right)_{T,p,\mu_i} \tag{4}$$

where p is the pressure and μ_i is the chemical potential of a chemical species, i. The capacitance of the liquid|liquid interface, C_{dl}, is then given by

$$C_{dl} = \left(\frac{\partial q^W}{\partial E}\right)_{T,p,\mu_i} = -\left(\frac{\partial^2\gamma}{\partial E^2}\right)_{T,p,\mu_i} \tag{5}$$

When a liquid–liquid two-phase system contains a surface-active ion, i, the adsorption of i around $\Delta_O^W\phi_i^{\circ}$ suppresses γ around $\Delta_O^W\phi_i^{\circ}$. Figure 3 shows the electrocapillary curve of a liquid–liquid two-phase system in the presence of the surface-active ion calculated by the model assuming that the two contributions to γ, the Gouy's electrical double layer[102] and the potential-dependent adsorption of the surface-active ion,[90] are independent.[45]

The dotted lines in Figures 3A and 3B are calculated electrocapillary curves in the absence of the surface active ion calculated based on the Gouy's electrical double layer model[102] on both side of the interface. This calculation assumes that 1:1 electrolytes exist in the both phases and the product of the concentration of the electrolyte and the relative permittivity of the media in each phase are $8\,\mathrm{mol\,dm^{-3}}$. The solid lines in Figures 3A and 3B are the electrocapillary curves in the presence of surface-active ions having $\beta_i = 0.5$ and 0.9, respectively. In the calculation of these curves, the adsorption is assumed to be described by the Frumkin isotherm, with the maximum adsorption of i at the interface being 5×10^{-6} $\mathrm{mol\,m^{-2}}$ and the point of zero charge in the absence of i being equal to $\Delta_O^W\phi_i^{\circ}$.[45]

The open circles in Figure 3 indicate the inflection points of the electrocapillary curves. Between these two points, $-0.05\,\mathrm{V} < \Delta_O^W\phi - \Delta_O^W\phi_i^{\circ} < 0.05\,\mathrm{V}$ in Figure 3A and $-0.09\,\mathrm{V} < \Delta_O^W\phi - \Delta_O^W\phi_i^{\circ} < 0.02\,\mathrm{V}$ in Figure 3B, the curvatures of the electrocapillary curves are positive. From eq 5, it is seen that the positive curvature of an electrocapillary curve means negative double layer capacitance, which is physically unrealistic. This condition, previously defined as the basis of electrochemical instability,[45] is a special case of the condition of the thermodynamic instability, $(\partial^2 G/\partial X^2) > 0$,[103] where G is a thermodynamic function and X is an intensive variable.

More precisely, for the stability, the system needs to satisfy the upward convexity of the electrocapillary curve, because γ is the excess surface Gibbs energy that determines the stability of the interface. The potential region where the interface becomes unstable due to the electrochemical instability should then be determined not by the inflection points on the electrocapillary curve but by the contact points (closed circles in Figure 3) between the electrocapillary curve and its common tangent line (broken lines in Figure 3).[83] Electrocapillary curves in the

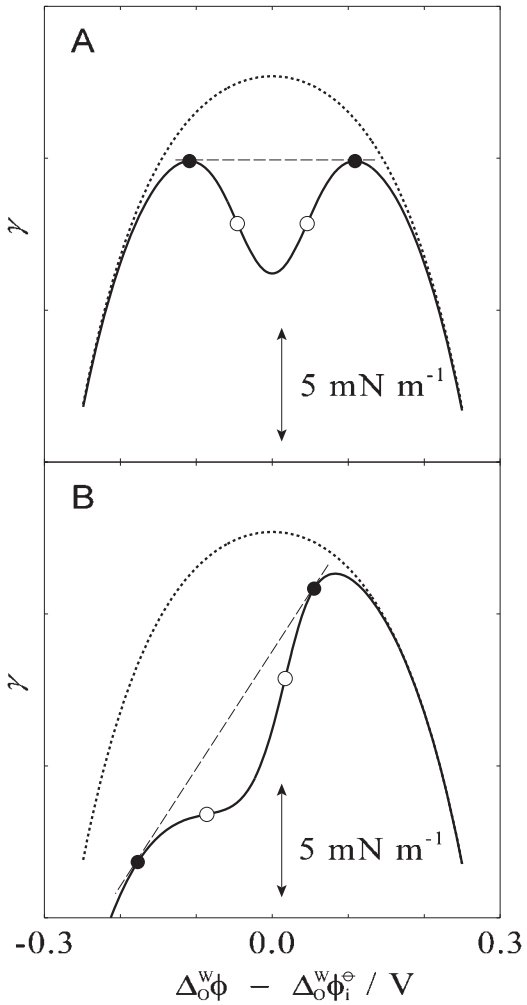

Figure 3. Electrocapillary curves in the absence (dotted lines) and presence of surface-active ion, i, (solid lines) having $\beta_i = 0.5$ (A) and 0.9 (B) when the product of the ionic strength and the relative permittivity of the solvent in each phase is 8 mol dm^{-3}, the maximum adsorption of i at the interface is 5×10^{-6} mol m^{-2}, and the point of zero charge in the absence of i is equal to $\Delta^{W}_{O}\phi^{\ominus}_{i}$. Open circles indicate the inflection points on the electrocapillary curves in the presence of surface-active ions. Broken lines are common tangent lines of the electrocapillary curves and closed circles show their contact points. Other conditions correspond to those in Figure 1.

presence of surface-active ion in Figures 3A and 3B show that the interface becomes unstable between −110 and 110 mV and between −230 and 60 mV, respectively.

Within this potential range, the interface becomes unstable to escape from this condition. The characteristic features of electrochemical instability are as follows. First, the instability appears in a certain potential region located near $\Delta^{W}_{O}\phi^{\ominus}_{i}$, that is, in the instability window. Second, γ at the potential just outside of the instability window is finite and positive, that is, the occurrence of the electrochemical instability is not associated with the ultralow γ. Third, the instability window widens with an increase in the concentration of the surface-active ion. Fourth, the instability window narrows with an increase in the concentration of the supporting electrolytes.

The model of the electrochemical instability proposed in 2002[45] explains the salient features of experimentally observed unstable phenomena. However, the assumption of this model, that is, the independence of the structure of the electrical double layer and the potential-dependent adsorption of the surface-active ion is inadequate except when the concentration of the surface-active ion is quite small. An improved model of the electrochemical instability that explicitly takes into account the effect of specifically adsorbed ions on the structures of the diffuse part of the double layer has recently been proposed.[104] The characteristic features of the electrochemical instability as mentioned above are confirmed in the improved model.[104]

5. Manifestations of the Electrochemical Instability

When a liquid–liquid two-phase system is under the electrochemical instability condition, a few different phenomena develop at the interface. This section presents the manifestations of the electrochemical instability in liquid–liquid two-phase systems, and the design of "spontaneous" instabilities at the liquid|liquid interface based on the electrochemical instability.

5.1 Voltammetric Manifestation of the Electrochemical Instability at the Liquid|Liquid Interface. Figure 4 shows voltammograms for the transfer of decylammonium across the DCE|W interface at the scan rates of 50 (A and B) and 10 mV s^{-1} (C) when the concentrations of decylammonium are 0.5 (A) and 1 mmol dm^{-3} (B and C).[83] The solid and broken lines in Figure 4 are voltammograms recorded in the absence and presence of sorbitan monooleate, which is known to suppress irregularly increased current,[81–83,85–88] in the DCE phase, respectively. The broken lines are close to regular voltammograms expected for a diffusion-limited current of decylammonium transfer. The solid lines show the irregularly increased current in the potential region around the midpoint potential (half-wave potential). Outside the potential region, the current is determined by the diffusion of decylammonium. In the potential region where the irregularly increased current appears, the DCE|W interface is under the electrochemical instability condition; the potential region widens with an increase in the concentration of the surface-active ion but the location is independent of the concentration (Figures 4A and 4B),[83,86,87] and the instability window determined by the voltammogram narrows with an increase in the concentration of the supporting electrolyte.[82] In addition, the increase in the scan rate causes the widening of the unstable potential region (Figures 4B and 4C).[81–83,86]

Similar irregularly increased currents are reported for the transfers of octanoate,[79] dicarboxylates,[80] alkylammoniums,[83,86,87] alkyl sulfates,[79,81,82,87,88] alkanesulfonates,[82,85] alkylimidazoliums,[83] and complexes of alkaline earth ions with surface-active neutral ligands.[84] The irregularly increased current observed for a variety of charged surface-active species suggests the generality of the electrochemical instability.

The abnormal increase of the current is caused by the hydrodynamic movement of the liquid phase adjacent to the interface due to the Marangoni effect.[81–83] The movement of the solution is suppressed at the micro liquid|liquid interfaces supported at the tip of a micropipette because of the small volume in the micropipette and the confinement of the interface at the tip.[86] The degree of the suppression increases with a

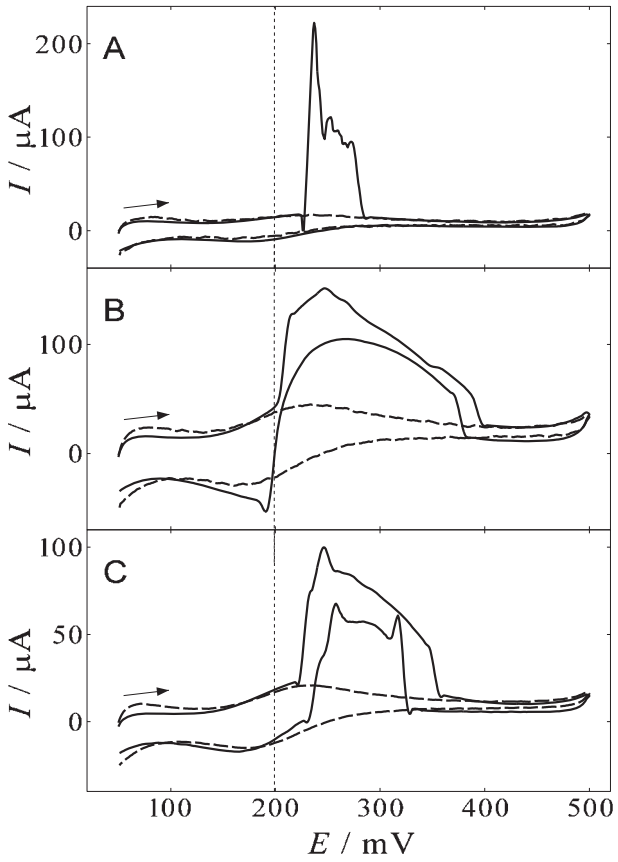

Figure 4. Voltammograms for the transfer of decylammonium across the DCE|W interface, when the concentrations of decylammonium are 0.5 (A) and 1 mmol dm^{-3} (B and C). The scan rates are 50 (A and B) and 10 mV s^{-1} (C). The supporting electrolytes are 100 mmol dm^{-3} LiCl and 10 mmol dm^{-3} HCl in the W phase and 100 mmol dm^{-3} tetrapentylammonium tetraphenylborate in the DCE phase. Broken lines are voltammograms recorded in the presence of 3 mmol dm^{-3} sorbitan monooleate in the DCE phase. The vertical line indicates the location of the midpoint potential of the voltammogram for the transfer of decylammonium. Adapted from Ref. 83 with permission.

decrease in the diameter at the tip of the micropipette, because the aspect ratio, that is, the depth per diameter of the capillary at the tip of a micropipette, increases with a decrease in the diameter. For example, normal diffusion-limited voltammograms for the transfer of decylammonium,[86] dodecanoate,[105] and perfluoroalkyl carboxylates and sulfonates[106] were obtained with a micropipette.

The characteristic features of the irregular current on the ion-transfer voltammogram are very similar to those seen in the polarographic maxima at the mercury electrode as described above. First, the irregular current appears around the half-wave potential of the polarogram.[61,66–68] Second, the irregular current is effectively suppressed by addition of the electrochemically inactive surfactant or gelatine.[66–68] Third, the irregular current, the movement of the liquid in the system, and the vibration of the interface continue while the potential is kept in the potential region where the polarographic maxima occur.[64,66,68] Fourth, when the potential is outside of the potential region exhibiting the polarographic maxima, the irregular current immediately disappears and the current drops to the value determined by the diffusion of the reactant.[62,63,68] These similarities suggest that the polarographic maximum and the irregularly increased current on the ion-transfer voltammogram have a common origin, that is, the coupling of the potential-dependent adsorption and the charge transfer across the interface, as Shikata suggested at the very beginning of the study of polarography.[61] At the mercury electrode, the charge transfer is a redox reaction accompanied with the adsorption of reactants or products or dissolution of the metal into mercury. At the O|W interface, the charge transfer is the partition of ions between the O and W phases.

5.2 Imaging the Evolution of Instability. It is important to understand when the interface enters into the mode of the electrochemical instability and how the incipient instability develops into instability of the entire interface. However, the voltammetry for the transfer of a surface-active ion provides no clue to these questions. To clarify the onset of the electrochemical instability, we observed with a confocal fluorescence microscope (CFM) the liquid|liquid interface under the potential control.[88]

Figure 5a shows voltammograms for the transfer of 1 mmol dm^{-3} dodecyl sulfate (DS^-) across the DCE|W interface in the presence of the adsorption of a fluorescent phosphatidylcholine at the scan rate of 100 mV s^{-1}.[88] The broken line in Figure 5a is a voltammogram recorded in the presence of sorbitan monooleate. Figure 5b shows the CFM images of the interface simultaneously recorded with the voltammogram shown in the solid line in Figure 5a. The alphabetical labels in Figure 5b correspond to those in Figure 5a indicating the potential when the image was acquired. In Figure 5b[A], the interface was homogeneously fluorescent. The dark domain with significantly weaker fluorescence appeared and grew slowly with scanning of the potential (Figures 5b[B]–5b[G]). In the potentials more negative than 300 mV, the dark domain grew rapidly and the movement of the domain continued while the irregular current was recorded (Figure 5b[H]). At $E = 150$ mV, the irregular current in the voltammogram disappeared in concurrence with the cessation of the movement. When $E < 150$ mV, the trace of the movement persisted as inhomogeneous fluorescence (Figure 5b[I]).

In Figure 5b, the dark domains are observed more negative than 360 mV. This potential is less positive than the potential at which the irregularly increased current appeared on the voltammogram in Figure 5a. In the potential region, 300 mV $< E <$ 360 mV, the interface was unstable but the irregularly increased current was not clearly discerned. In this potential range, interestingly, the interface appears to be globally stable at the expense of small unstable domains. In other words, the large stable region and the locally unstable domains coexist in a globally metastable state.[88]

5.3 Spontaneous Emulsification as a Manifestation of the Electrochemical Instability. Since Gad advocated the importance of spontaneous emulsification of fat in contact with alkaline media in 1878,[1] spontaneous emulsification has been reported in a variety of conditions, for example, oil–water two-phase systems in the presence of nonionic surfactants,[6,9,15,17,18,21–23] anionic surfactants,[1–5,7,8,10–13,16,19,20] cationic surfactants,[6] nonsurface active salts,[25] and in the liquid–

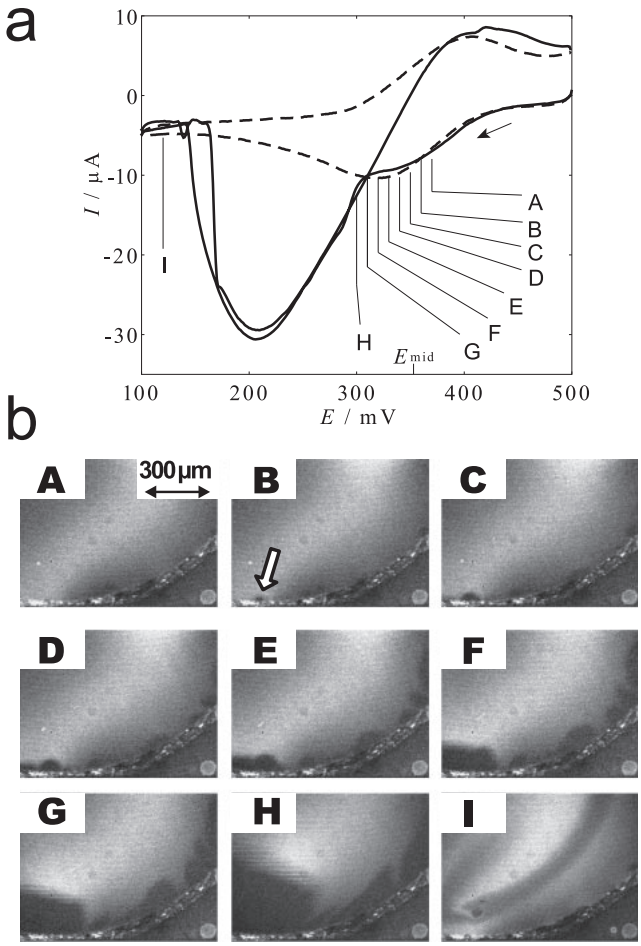

Figure 5. Voltammograms for the transfer of 1 mmol dm^{-3} dodecyl sulfate across the DCE|W interface in the presence of the fluorescent phospholipid (D3815, Molecular Probes) at the scan rate of 100 mV s^{-1} (a) and simultaneously recorded images of the DCE|W interface by using a confocal fluorescence microscope (b). The solid and dotted lines indicate the voltammograms recorded in the absence and presence of 1 mmol dm^{-3} sorbitan monooleate in the DCE phase, respectively. The alphabets in the images correspond to those in the voltammogram. The arrow in image B points the dark domain that appeared. Adapted from Ref. 88 with permission.

liquid two-phase systems containing no solute.[24] In particular, the emulsification induced in the presence of ionic surfactants is likely to be related to the electrochemical instability. The electrochemical instability has been studied under the external control of $\Delta_O^W\phi$ as described above.[81–88] However, at any liquid|liquid interface in nature, $\Delta_O^W\phi$ is determined without electrodes by the distribution of ions[107–110] and/or its conjugation with redox reactions.[111] It is therefore possible to control $\Delta_O^W\phi$ across the liquid|liquid interface without electrodes. If $\Delta_O^W\phi$ is adjusted to be in the instability window and the electrochemical instability emerges without the externally applied voltage, the emulsification would appear to be spontaneous.

When a liquid–liquid two-phase system is at the partition equilibrium, $\Delta_O^W\phi$ is uniquely determined by the activities and $\Delta_O^W\phi_i^\ominus$ values of the ionic components.[108–110] Following is an

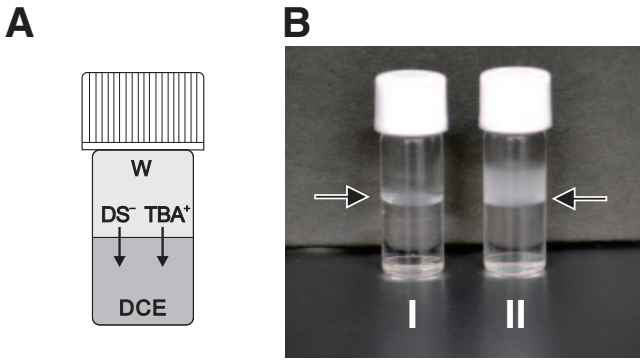

Figure 6. Schematic view of the DCE–W two-phase system containing TBADS (A). DCE–W two-phase systems after 1 (I) and 7 min (II) contact of the aqueous solution of 2.5 mmol dm^{-3} TBADS with DCE (B). Arrows in B point the positions of the DCE|W interface.

example of the design of a DCE–W two-phase system that undergoes spontaneous emulsification. In the system shown in Figure 6A, $\Delta_O^W\phi$, which is determined by the partition of tetrabutylammonium dodecyl sulfate (TBADS), is located within the instability window determined by the adsorption and partitioning of DS^-.[112] Figure 6B shows the spontaneous emulsification at the interface between the aqueous solution of 2.5 mmol dm^{-3} TBADS and DCE 1 (I) and 7 min (II) after the contact of the two solutions. Arrows in Figure 6B indicate the location of the interface. In Figure 6B, the spontaneously formed emulsion was observed in the W phase. This result demonstrates that the spontaneous emulsification can be designed based on the electrochemical instability. Since the DCE and the aqueous phases were mutually saturated before use in this experiment, the transfer of the surfactant across the interface for the partition equilibrium is only the possible driving force of this emulsification. Although spontaneously formed emulsions are highly stable in general,[3,4,6,7,10,14,17,21] the emulsions induced by TBADS disappeared after a few hours. This low stability of the emulsions may be due to the relatively high γ at the DCE|W interface. The reason why emulsions appear only in the W phase in this system remains to be explained.

The spontaneous emulsification induced by a single ionic surfactant[4–8,10,11,13,16,19,20] would be explained by the electrochemical instability as the same manner as TBADS. In the spontaneous emulsification accompanied with the chemical reaction of ionic surfactants at the interface,[1–3,5,12] $\Delta_O^W\phi$ is probably located in the instability window due to the partition and adsorption of the surface-active ion and the energy of the chemical reaction may drive the spontaneous emulsification.

The switching of the spontaneous emulsification depending on $\Delta_O^W\phi$ has been found in the ionic liquid–water two-phase system.[113] This emulsification is an example of the electrochemical instability at the ionic liquid|water interface.

The spontaneous emulsification caused by nonionic surfactants[6,9,15,17,18,21–23] is outside of the realm of the electrochemical instability. However, nonionic surfactants having oligooxyethylene moiety as the hydrophilic part may work as cationic surfactants through the complexation with the metal ions,[114–117] which renders some nonionic surfactant systems responsive to $\Delta_O^W\phi$.

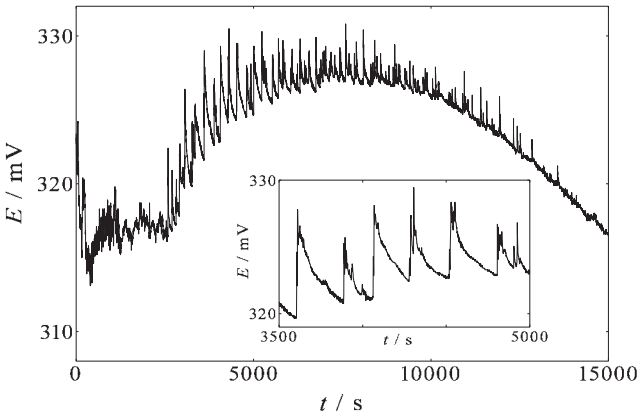

Figure 7. The oscillation of the potential of a cell in the presence of 20 mmol dm^{-3} TPADS and 10 mmol dm^{-3} LiCl in W and 10 mmol dm^{-3} tetrapentylammonium tetraphenylborate in DCE. The inset shows the magnified view between 3500 and 5000 s.

5.4 Oscillation Phenomena Caused by the Electrochemical Instability. Another well-known instability, the spontaneous oscillation of $\Delta_O^W\phi$ in the liquid–liquid two-phase system, can be understood in terms of the electrochemical instability. To demonstrate the significance of the electrochemical instability in oscillation phenomena, we designed a DCE–W two-phase system containing tetrapropylammonium dodecyl sulfate (TPADS). The distribution of TPADS in the DCE–W two-phase system can set the value of $\Delta_O^W\phi$ within the instability window in the same manner as TBADS.[112]

A typical oscillation of $\Delta_O^W\phi$ between the aqueous solution of TPADS and DCE is shown as the oscillation of E in Figure 7.[118] In this example, the oscillation of E started after an induction period of about 2500 s. The inset of Figure 7 is the magnified view of the region of $3500\,\text{s} < t < 5000\,\text{s}$. The oscillation has a period of about 250 s and an amplitude of about 5 mV. The waveform of the oscillation is asymmetric, with the positive change of E for about 10 s and the negative change of E for about 240 s. The simultaneous γ measurement shows that the positive change in E corresponds to the adsorption of DS^- (data not shown).[118]

The oscillation of $\Delta_O^W\phi$ at the DCE|W interface was achieved on the basis of the electrochemical instability. The reported oscillation of $\Delta_O^W\phi$ in the systems containing DS^- and tetrabutylammonium[31,38,42] would also be caused by the electrochemical instability. However, the connection of the electrochemical instability with oscillations of $\Delta_O^W\phi$ and γ accompanied with the interfacial reactions[26–29,33–37,39–41] is far from persuasive. In addition, three fundamental questions remain unanswered in the oscillation phenomena that seem to be within the framework of the electrochemical instability. The first question is the origin of the oscillation of $\Delta_O^W\phi$ which has a period of 250 s. A model taking into account the formation and destruction of the surfactant layer at the interface[33,35,38] disagrees with this slow oscillation because the concentration of TBADS is high enough to restore the concentration profile in the vicinity of the interface in such a long period of time. The second question is why locally unstable submillimeter-scale domains at the interface at the incipient stage of the electrochemical instability[88] collaborate to create a rhythm that concerts with each other over the entire interface spontaneously. The third question is why the induction period of a few minute is required. In the oscillation in the liquid membrane system, the induction period has been explained by the diffusion of surfactant across the liquid membrane.[35,38,42] Such an induction period seems to always precede the oscillation even in the oil–water two-phase system.[28,31,118]

5.5 The Effect of Nonionic Surfactant on the Electrochemical Instability. Although the addition of sorbitan monooleate suppressed the emergence of the irregular current on the voltammogram, the heterogeneity of the interface was observed in CFM images when sorbitan monooleate was added into the system.[88] Thus, the locally confined electrochemical instability is present even in the presence of sorbitan monooleate. The addition of sorbitan monooleate in the oil phase lowers γ in the entire potential region[119] and also decreases the potential dependence of γ in the presence of surface-active ion.[83,85,87] The local gradient of γ when the interface is under the electrochemical instability condition would then become smaller and so is the driving force for the Marangoni instability. The effect of the addition of the electrochemically inactive surfactant on the mercury dropping electrode to suppress the polarographic maxima seems to be explained in the same manner.

6. Conclusion

The electrochemical instability clarifies the conditions of the appearance and disappearance of unstable phenomena at the liquid|liquid interface, such as the irregularly increased current on the ion-transfer voltammogram, the spontaneous oscillation of $\Delta_O^W\phi$ and γ, and the spontaneous emulsification. In these interesting and important phenomena, $\Delta_O^W\phi$ is the key parameter to understand and to control the instability. Examples of controlling the instability by applying the potential externally or by adjusting the composition of the ions in the system described above demonstrate that the electrochemical instability is a fundamental concept that determines the condition for the stability at liquid|liquid interfaces, which is inevitably electrified. Problems that remain unanswered in relation to the instability at the liquid|liquid interface have been delineated.

This work was partially supported by a Grant-in-Aid for Scientific Research (No. 21245021) from the Ministry of Education, Culture, Sports, Science and Technology, Japan. The support by the Global COE program "International Center for Integrated Research and Advanced Education in Materials Science" (No. B-09) from the Ministry of Education, Culture, Sports, Science and Technology, Japan, is highly appreciated.

References

1 J. Gad, *Arch. Anat. Physiol.* **1878**, 181.
2 G. Quincke, *Ann. Phys.* **1888**, *271*, 580.
3 J. W. McBain, T.-M. Woo, *Proc. R. Soc. London, Ser. A* **1937**, *163*, 182.
4 J. W. McBain, T. M. Woo, *J. Phys. Chem.* **1938**, *42*, 1099.
5 A. C. Frazer, J. H. Schulman, H. C. Stewart, *J. Physiol.* **1944**, *103*, 306.
6 A. Kaminski, J. W. McBain, *Proc. R. Soc. London, Ser. A* **1949**, *198*, 447.

7 M. J. Groves, *Chem. Ind.* **1978**, *17*, 417.
8 H. Kunieda, K. Shinoda, *J. Colloid Interface Sci.* **1979**, *70*, 577.
9 C. W. Pouton, *Int. J. Pharm.* **1985**, *27*, 335.
10 R. W. Greiner, D. F. Evans, *Langmuir* **1990**, *6*, 1793.
11 A. Shioi, M. Harada, K. Matsumoto, *J. Phys. Chem.* **1991**, *95*, 7495.
12 J. Rudin, D. T. Wasan, *Chem. Eng. Sci.* **1993**, *48*, 2225.
13 J. Eastoe, T. F. Towey, B. H. Robinson, J. Williams, R. K. Heenan, *J. Phys. Chem.* **1993**, *97*, 1459.
14 P. P. Constantinides, *Pharm. Res.* **1995**, *12*, 1561.
15 H. Kunieda, Y. Fukui, H. Uchiyama, C. Solans, *Langmuir* **1996**, *12*, 2136.
16 N. Shahidzadeh, D. Bonn, J. Meunier, *Europhys. Lett.* **1997**, *40*, 459.
17 M. J. Rang, C. A. Miller, *Prog. Colloid Polym. Sci.* **1998**, *109*, 101.
18 N. Shahidzadeh, D. Bonn, J. Meunier, M. Nabavi, M. Airiau, M. Morvan, *Langmuir* **2000**, *16*, 9703.
19 T. Nishimi, C. A. Miller, *Langmuir* **2000**, *16*, 9233.
20 M. Nakagawa, N. Sezaki, T. Kakiuchi, *J. Electroanal. Chem.* **2001**, *501*, 260.
21 J. C. López-Montilla, P. E. Herrera-Morales, S. Pandey, D. O. Shah, *J. Dispersion Sci. Technol.* **2002**, *23*, 219.
22 V. K. Srivastava, G. Kini, D. Rout, *J. Colloid Interface Sci.* **2006**, *304*, 214.
23 V. I. Uricanu, M. H. G. Duits, D. Filip, R. M. F. Nelissen, W. G. M. Agterof, *J. Colloid Interface Sci.* **2006**, *298*, 920.
24 K. Tauer, S. Kozempel, G. Rother, *J. Colloid Interface Sci.* **2007**, *312*, 432.
25 K. Aoki, M. Li, J. Chen, T. Nishiumi, *Electrochem. Commun.* **2009**, *11*, 239.
26 M. Dupeyrat, E. Nakache, *Bioelectrochem. Bioenerg.* **1978**, *5*, 134.
27 A. Shioi, K. Katano, Y. Onodera, *J. Colloid Interface Sci.* **2003**, *266*, 415.
28 D. Lavabre, V. Pradines, J.-C. Micheau, V. Pimienta, *J. Phys. Chem. B* **2005**, *109*, 7582.
29 A. Shioi, Y. Sugiura, R. Nagaoka, *Langmuir* **2000**, *16*, 8383.
30 N. M. Kovalchuk, D. Vollhardt, *Adv. Colloid Interface Sci.* **2006**, *120*, 1.
31 V. Pradines, R. Tadmouri, D. Lavabre, J.-C. Micheau, V. Pimienta, *Langmuir* **2007**, *23*, 11664.
32 K. Wojciechowski, M. Kucharek, *J. Phys. Chem. B* **2009**, *113*, 13457.
33 K. Yoshikawa, Y. Matsubara, *J. Am. Chem. Soc.* **1983**, *105*, 5967.
34 K. Maeda, S. Kihara, M. Suzuki, M. Matsui, *J. Electroanal. Chem. Interfacial Electrochem.* **1990**, *295*, 183.
35 K. Arai, F. Kusu, K. Takamura, *Chem. Lett.* **1990**, 1517.
36 H. Suzuki, Y. Tsuchiya, T. Kawakubo, *Biophys. Chem.* **1991**, *40*, 149.
37 S. Kihara, K. Maeda, *Prog. Surf. Sci.* **1994**, *47*, 1.
38 K. Arai, S. Fukuyama, F. Kusu, K. Takamura, *Electrochim. Acta* **1995**, *40*, 2913.
39 S. Sutou, H. Yoshihisa, K. Miyamura, Y. Gohshi, *J. Colloid Interface Sci.* **1997**, *187*, 544.
40 K. Maeda, S. Nagami, Y. Yoshida, H. Ohde, S. Kihara, *J. Electroanal. Chem.* **2001**, *496*, 124.
41 V. Pimienta, R. Etchenique, T. Buhse, *J. Phys. Chem. A* **2001**, *105*, 10037.
42 T. Ogawa, H. Shimazaki, S. Aoyagi, K. Sakai, *J. Membr. Sci.* **2006**, *285*, 120.
43 J. B. Lewis, H. R. C. Pratt, *Nature* **1953**, *171*, 1155.
44 T. Sherwood, J. Wei, *Ind. Eng. Chem.* **1957**, *49*, 1030.
45 T. Kakiuchi, *J. Electroanal. Chem.* **2002**, *536*, 63.
46 C. A. Miller, L. E. Scriven, *J. Colloid Interface Sci.* **1970**, *33*, 360.
47 A. Paalzow, *Ann. Phys.* **1858**, *180*, 413.
48 G. Lippmann, *Ann. Phys.* **1873**, *225*, 546.
49 G. Kučera, *Ann. Phys.* **1903**, *316*, 529.
50 C. V. Sternling, L. E. Scriven, *AIChE J.* **1959**, *5*, 514.
51 B. Gross, A. N. Hixson, *Ind. Eng. Chem. Fundam.* **1969**, *8*, 289.
52 P. L. T. Brian, *AIChE J.* **1971**, *17*, 765.
53 M. Hennenberg, P. M. Bisch, M. Vignes-Adler, A. Sanfeld, *J. Colloid Interface Sci.* **1979**, *69*, 128.
54 M. A. Mendes-Tatsis, E. S. Perez De Ortiz, *Chem. Eng. Sci.* **1996**, *51*, 3755.
55 S. Slavtchev, M. Hennenberg, J.-C. Legros, G. Lebon, *J. Colloid Interface Sci.* **1998**, *203*, 354.
56 S. Slavtchev, P. Kalitzova-Kurteva, M. A. Mendes, *Colloids Surf., A* **2006**, *282–283*, 37.
57 J. R. A. Pearson, *J. Fluid Mech.* **1958**, *4*, 489.
58 P. Colinet, J. C. Legros, M. G. Velarde, *Nonlinear Dynamics of Surface-Tension-Driven Instabilities*, Wiley-VCH, Berlin, **2001**.
59 R. Parsons, in *Modern Aspects of Electrochemistry*, ed. by J. O. Bockris, B. E. Conway, Butterworths, London, **1954**, Chap. 3.
60 J. O. Bockris, A. K. N. Reddy, M. Gamboa-Aldeco, *Modern Electrochemistry*, 2nd ed., Kluwer Academic/Plenum Publishers, New York, **2000**.
61 M. Shikata, *Trans. Faraday Soc.* **1925**, *21*, 42.
62 N. V. Emelianova, J. Heyrovský, *Trans. Faraday Soc.* **1928**, *24*, 257.
63 D. Ilkovič, *Collect. Czech. Chem. Commun.* **1936**, *8*, 13.
64 H. J. Antweiler, *Z. Elektrochem. Angew. Phys. Chem.* **1938**, *44*, 719.
65 A. Frumkin, *J. Colloid Sci.* **1946**, *1*, 277.
66 I. M. Kolthoff, J. J. Lingane, *Polarography*, 2nd ed., Interscience Publishers, New York, **1952**.
67 J. Heyrovský, J. Kůta, *Principles of Polarography*, Academic Press, Inc., New York, **1966**.
68 H. H. Bauer, *Streaming Maxima in Polarography* in *Electroanalytical Chemistry*, ed. by A. J. Bard, Marcel Dekker, Inc., New York, **1975**, Vol. 8.
69 E. L. Colichman, *J. Am. Chem. Soc.* **1952**, *74*, 722.
70 C. A. Streuli, W. D. Cooke, *Anal. Chem.* **1953**, *25*, 1691.
71 J. Y. Becker, G. Ginzburg, I. Willner, *J. Electroanal. Chem.* **1980**, *108*, 355.
72 M. S. Saha, Y. Che, T. Okajima, T. Kiguchi, Y. Nakamura, K. Tokuda, T. Ohsaka, *J. Electroanal. Chem. Interfacial Electrochem.* **2001**, *496*, 61.
73 M. E. Ortiz, L. J. Núñez-Vergara, J. A. Squella, *J. Electroanal. Chem.* **2002**, *519*, 46.
74 Md. M. Islam, M. T. Alam, T. Okajima, T. Ohsaka, *J. Phys. Chem. B* **2007**, *111*, 12849.
75 J. Guastalla, *J. Chim. Phys.* **1956**, *53*, 470.
76 M. Blank, *J. Colloid Interface Sci.* **1966**, *22*, 51.
77 C. Gavach, P. Seta, F. Henry, *Bioelectrochem. Bioenerg.* **1974**, *1*, 329.
78 J. Koryta, P. Vanýsek, M. Bŕezina, *J. Electroanal. Chem.*

Interfacial Electrochem. **1976**, *67*, 263.
79 P. Vanýsek, *J. Electroanal. Chem.* **1981**, *121*, 149.
80 Y. Shao, S. G. Weber, *J. Phys. Chem.* **1996**, *100*, 14714.
81 T. Kakiuchi, M. Chiba, N. Sezaki, M. Nakagawa, *Electrochem. Commun.* **2002**, *4*, 701.
82 T. Kakiuchi, N. Nishi, T. Kasahara, M. Chiba, *ChemPhysChem* **2003**, *4*, 179.
83 T. Kasahara, N. Nishi, M. Yamamoto, T. Kakiuchi, *Langmuir* **2004**, *20*, 875.
84 T. Kakiuchi, *J. Electroanal. Chem.* **2004**, *569*, 287.
85 T. Sakka, K. Tanaka, Y. Shibata, Y. H. Ogata, *J. Electroanal. Chem.* **2006**, *591*, 168.
86 Y. Kitazumi, T. Kakiuchi, *J. Phys.: Condens. Matter* **2007**, *19*, 375104.
87 Y. Kitazumi, T. Kakiuchi, *Langmuir* **2009**, *25*, 8062.
88 Y. Kitazumi, T. Kakiuchi, *Langmuir* **2009**, *25*, 10829.
89 L. I. Daikhin, M. Urbakh, *J. Chem. Phys.* **2008**, *128*, 014706.
90 T. Kakiuchi, *J. Electroanal. Chem.* **2001**, *496*, 137.
91 T. Kakiuchi, M. Kobayashi, M. Senda, *Bull. Chem. Soc. Jpn.* **1987**, *60*, 3109.
92 T. Kakiuchi, M. Kobayashi, M. Senda, *Bull. Chem. Soc. Jpn.* **1988**, *61*, 1545.
93 D. C. Grahame, *J. Am. Chem. Soc.* **1958**, *80*, 4201.
94 R. Parsons, *Trans. Faraday Soc.* **1959**, *55*, 999.
95 M. Gros, S. Gromb, C. Gavach, *J. Electroanal. Chem. Interfacial Electrochem.* **1978**, *89*, 29.
96 T. Kakiuchi, M. Senda, *Bull. Chem. Soc. Jpn.* **1983**, *56*, 1753.
97 H. H. J. Girault, D. J. Schiffrin, B. D. V. Smith, *J. Colloid Interface Sci.* **1984**, *101*, 257.
98 M. C. Martins, C. M. Pereira, H. H. Girault, F. Silva, *Electrochim. Acta* **2004**, *50*, 135.
99 A. Lhotský, V. Mareček, S. Zális, Z. Samec, *J. Electroanal. Chem.* **2005**, *585*, 269.
100 J. Koryta, P. Vanýsek, M. Březina, *J. Electroanal. Chem. Interfacial Electrochem.* **1977**, *75*, 211.
101 G. Lippmann, *Ann. Chim. Phys.* **1875**, *5*, 494.
102 G. Gouy, *Ann. Chim. Phys.* **1917**, *7*, 129.
103 J. W. Gibbs, *The Scientific Papers of J. Willard Gibbs*, Longmans, Green, and Co., London, **1906**, Vol. 1.
104 Y. Kitazumi, T. Kakiuchi, *J. Electroanal. Chem.* **2010**, *648*, 8.
105 P. Jing, M. Zhang, H. Hu, X. Xu, Z. Liang, B. Li, L. Shen, S. Xie, C. M. Pereira, Y. Shao, *Angew. Chem., Int. Ed.* **2006**, *45*, 6861.
106 P. Jing, P. J. Rodgers, S. Amemiya, *J. Am. Chem. Soc.* **2009**, *131*, 2290.
107 R. Luther, *Z. Phys. Chem.* **1896**, *19*, 529.
108 L. Q. Hung, *J. Electroanal. Chem. Interfacial Electrochem.* **1980**, *115*, 159.
109 L. Q. Hung, *J. Electroanal. Chem. Interfacial Electrochem.* **1983**, *149*, 1.
110 T. Kakiuchi, *Anal. Chem.* **1996**, *68*, 3658.
111 T. Kakiuchi, *Electrochim. Acta* **1995**, *40*, 2999.
112 Y. Kitazumi, T. Kakiuchi, in preparation.
113 S. Suzuki, Y. Kitazumi, T. Kakiuchi, in preparation.
114 Z. Yoshida, S. Kihara, *J. Electroanal. Chem.* **1987**, *227*, 171.
115 T. Kakiuchi, T. Usui, M. Senda, *Bull. Chem. Soc. Jpn.* **1990**, *63*, 2044.
116 T. Kakiuchi, T. Usui, M. Senda, *Bull. Chem. Soc. Jpn.* **1990**, *63*, 3264.
117 T. Kakiuchi, *J. Colloid Interface Sci.* **1993**, *156*, 406.
118 Y. Kitazumi, J. Uchiyashiki, T. Kakiuchi, in preparation.
119 T. Kakiuchi, Y. Teranishi, K. Niki, *Electrochim. Acta* **1995**, *40*, 2869.

Takashi Kakiuchi graduated Department of Agricultural Chemistry, Kyoto University, in 1971, and received Dr.Agr. in 1978 at Kyoto University. After 15 years in the same department, he moved to Yokohama National University as Associate Professor in Department of Physical Chemistry in 1993 and was prompted to Professor in 1997. He moved to Department of Energy and Hydrocarbon Chemistry, Graduate School of Engineering, Kyoto University, in 1998. His research interests include instability phenomena at fluid interfaces, electrochemistry of ionic liquids, and electroanalytical chemistry, in general.

Yuki Kitazumi was born in 1981 in Gunma, Japan. He graduated from Gunma National College of Technology in 2002 and received his B.Eng. (2005), M.Eng. (2007), and Ph.D. (2010) degrees from Kyoto University. He joined the faculty at Kyoto University as assistant professor in 2010. His research interests focus on ionic surfactants and instabilities at the liquid|liquid interface.